Identification process based on shear wave propagation within a phantom using finite element modelling and magnetic resonance elastography

Gwladys Leclerc, Fabrice Charleux, Marie-Christine Ho Ba Tho, Sabine Bensamoun

Identification process based on shear wave propagation within a phantom using finite element modelling and magnetic resonance elastography

Gwladys E. Leclerc[1]
Fabrice Charleux[2]
Marie-Christine Ho Ba Tho[1]
Sabine F. Bensamoun[1]

[1]Université de Technologie de Compiègne, UMR CNRS 7338, BioMécanique et BioIngénierie, Compiègne, France
[2]ACRIM-Polyclinique Saint Côme, Compiègne, France

Original article
Word count: 3130

Corresponding author

Dr Sabine F. Bensamoun, PhD

Université de Technologie de Compiègne (UTC)
Centre de Recherches de Royallieu
Laboratoire de BioMécanique et BioIngénierie, UMR CNRS 7338
Rue Personne de Roberval
BP 20529
60205 Compiègne Cedex
France
Tel : (33) 03 44 23 43 90
Email: sabine.bensamoun@utc.fr

Identification process based on shear wave propagation within a phantom using finite element modelling and magnetic resonance elastography

Original article

Word count: 3130

Abstract

Magnetic resonance elastography (MRE), based on shear wave propagation, is a non-invasive clinical exam, improving the diagnosis of liver disorders. The purpose of this study was to develop a finite element (FE) model simulating the wave displacement within a phantom, having a similar liver stiffness, using the realistic MRE liver boundary conditions (frequency, displacement of the membrane constituted the liver driver).

A 3D finite element model, composed of the exciting membrane of the liver driver and the phantom, was developed with the software ABAQUS. Different ranges of mesh size, density and Poisson's ratio were tested in order to develop the most representative FE phantom model for liver tissue. The simulated wave displacement was visualized with a dynamic implicit analysis. Subsequently, an identification process was made with a cost function and an optimization loop provided the optimal elastic properties of the phantom.

The similar experimental (MRE) and numerical (FE) wave displacement validates the present identification process performed on a phantom which is comparable to a fibrotic liver. This study provides experimental and numerical data related to MRE technique which could be used in the future as a starting point for the development of finite element models mimicking various abdominal tissue behaviors.

Key Words: Magnetic Resonance Elastography; Finite Element Modelling; Phantom; Identification process; Mechanical properties

I. INTRODUCTION

Clinical diagnosis established from imaging tests (MRI, CT scan, Ultrasound) are primarily based on an analysis of the structural properties of the tissue represented by its texture and morphology [1,2]. In addition to the common anatomical acquisition, a second image can now revealed the cartography of the tissue stiffness, provided by clinical elastography techniques [3–6]. Thus, the association of the morphological and mechanical properties of the tissue have allowed the clinician to better diagnose, in a non-invasive way, the pathology, such as the stage of fibrosis in the liver [7]. To further improve the medical diagnosis, the structural and functional properties were then implemented in constitutive models in order to accurately simulate the tissue behavior used for surgery training and planning [8,9].

Finite element modelling (FEM) was associated with clinical imaging techniques, such as elastography techniques, which are based on the shear wave propagation within the soft tissue in order to simulate the wave displacement. Thus, the V-shape wave patterns observed in the biceps brachii along the direction of muscle fibers was simulated through 3D coupled harmonic oscillator calculations [10] including the muscle morphology. In addition to the simulation of complex wave patterns, computer models were used to simulate in vivo experiments in order to provide an evaluation of the method. Indeed, in vivo MR elastography protocols can be difficult to set up for certain organs including the brain [11,12] or for the analysis of the atherosclerotic plaque [13].

Since 1995 [14], the MR elastography technique has demonstrated its capability to measure the mechanical properties of a large range of soft tissue (muscle, cartilage, lung, heart, carotid artery) and was recently recognized as a clinical test for the liver. In order to implement other MRE clinical protocols, finite element modelling was used to determine the feasibility of the MR elastography method to characterize the eye [15] and the brain [12].

In parallel to *in vivo* experiments performed with MR elastography (MRE), finite element (FE) simulation was used for the validation of the MRE stiffness measurement [11] through the development of different types of gel phantoms (bovine, agarose, and wirosil). Furthermore, phantoms were composed of taut band [16] to mimic the wave patterns within the trapezius muscle, or made with inclusions [17] to simulate the tissue behavior within breast cancer. In addition, various boundary conditions of MR elastography technique can be tested on a phantom before applying to *in vivo* experiments, and the use of FE modelling aids in understand the shear wave behavior [18,19] leading to the stiffness tissue measurement.

Thus, the purpose of the present study was to simulate the shear wave propagation within a phantom, created with a stiffness similar to a fibrotic liver, using the clinical liver MR elastography protocol and a finite element model composed of realistic liver MRE boundary conditions [20]. To achieve this aim, an identification process, based on the comparison of the experimental (MRE) and numerical (FE) results, was developed and this method could be used in the future for the functional characterization of other abdominal tissues, improving the diagnostic procedures and the follow-up of the effects of treatments.

II. MATERIALS AND METHODS

2.1 In vivo and in vitro MRE tests performed on liver tissue and phantom

A. Healthy and fibrotic liver tissues

Ten healthy subjects and 10 patients currently enrolled in alcohol dependence programs were recruited at the alcoholism department. The study was approved by the Institutional Review Board and written informed consent was obtained.

The following MRE protocol has been standardized to be currently used in Europe and the United State as a clinical exam [21]. The subjects lay supine on a 1.5T Signa HDx MRI machine (General Electric, Milwaukee, WI, USA) and the center of a cylindrical pneumatic driver (diameter: 16 cm) was placed at the same level as the diaphragm and positioned in contact with the rib cage (Fig. 1A). The body coil was used and the driver had a long hose connected to an active loudspeaker. This system created time-varying pressure waves propagating shear waves within the abdomen at the frequency (f) of 60 Hz. MRE images were collected with a motion-sensitized gradient-echo sequence, at two time offsets (phase offsets) between the start of the motion and the motion encoding gradients, using a single number of gradients. Two offsets were recorded in a row, and during this acquisition the subjects held their breathing to avoid the motion of the liver caused by the displacement of the diaphragm. The total scan time recorded was 32s corresponding to 2 breath-holding periods of 16s.

The acquisition matrix was 256x64 (which was interpolated to 256x256), the flip angle was 30°, the field of view was between 36 and 48 cm as a function of the morphology of the subject. According to the MRE parameters, the TR was 100 ms and the TE corresponded to the minimum echo time (26.8 ms) that allowed for motion encoding.

MRE axial images were recorded for each subject and phase images (Fig. 1B, 1C) showed the shear wave displacement within the healthy and the fibrotic liver tissues. Then, a profile was manually placed in the direction of the wave propagation and the wavelength (λ) was measured as the distance between two consecutive peaks (Fig. 1D). The elastic properties (shear stiffness: μ) of the livers were calculated with the following equation: $\mu = \rho\lambda^2 f^2$ (ρ = 1000 kg/m^3 the liver density). It is assumed that the liver is composed of an isotropic, a homogeneous and an elastic media. Repeatability of MRE acquisitions was conducted on each subject, on the same day but at different times.

B. Phantom

The MRE experimental boundary conditions (frequency, displacement of the membrane constituted the liver driver) applied to the phantom was the same as those prescribed previously for the liver MRE test in order to simulate the shear wave propagation within the hepatic gland. It must be noted that the following protocol was described in a previous study [20] and is briefly summarized here. A homogeneous phantom (diameter = 25 cm, height = 5 cm), composed of 45% softener and 55% liquid plastic (LureCraft, LaGrande, USA was created with the aim of obtaining a phantom whose media was similar to a fibrotic liver stiffness, allowing for mimicking of this tissue. The phantom was placed inside a 1.5T MRI machine (GE, Signa HDx) and shear waves were generated through the phantom by the same cylindrical pneumatic driver used for the MRE clinical liver exam (Fig. 2A). This driver is composed of a thin flexible membrane (10-20 μm) made of polycarbonate enclosed by rigid walls [22] and the maximal displacement of the membrane was 39.2 μm for a frequency (f) of 60Hz [20]. A head coil was used and MRE images were collected with a gradient echo sequence, a flip angle of 45°, a 30x30 cm field of view and a 256x64 acquisition matrix. Four offsets were recorded with a TE corresponding to the minimum echo time allowing for motion encoding and a TR equal to

50 ms. MRE technique provided phase images (Fig. 2B) showing the shear wave displacement within the phantom. Similar to the liver tissue analysis, a profile was manually placed in the radial direction of the shear wave propagation. The wavelength (λ) was measured as the distance between two consecutive peaks, and the elastic property (shear stiffness: μ) of the phantom was calculated with the following equation: $\mu = \rho\lambda^2 f^2$ (ρ = 1000 kg/m^3 the density of the phantom). It is also assumed that the phantom is composed of an isotropic, homogeneous and elastic media.

2.2 Finite element (FE) models

To simulate the propagation of the shear wave through the phantom, a 3D finite element model, composed of two FE models represented by the exciting membrane of the liver driver (Fig. 2C) and the phantom (Fig. 2D), was developed with the software ABAQUS 6.9-1 Standard (Simulia Dassault Systems).

The FE element model of the membrane was represented with the same material properties and boundary conditions as the one which constituted the MRE liver clinical exam (Fig. 1A). Thus, a cylindrical shell with a 16 cm diameter (R: radius) and a 10 μm thickness (e) [22] were numerically generated (Fig. 2C). The membrane was meshed with S4R (4-node shell) elements of 10 mm and the prescribed mechanical properties were taken from the literature [23] and fixed to 2400 MPa for the Young's modulus (E), to 0.37 for the Poisson's ratio (ν), and 1200 kg/m^3 for the density (ρ).Realistic boundary conditions were imposed to the membrane's model, i.e. edges clamped, a mechanical excitation at 60 Hz with the corresponding vertical displacement (U_z) imposed on each node (Fig. 2C). This displacement was obtained from the theoretical bending definition for a cylindrical, isotropic, homogenenous plate subjected to a uniform pressure (P, MPa) with clamped edges in cylindrical coordinates, associated with a bending rigidity (D, N.m):

$$U_Z(r) = \frac{P}{64D}\left(r^4 - 2r^2R^2 + R^4\right) \text{ with } D = \frac{E\ e^3}{12\left(1-\nu^2\right)} \quad (1)$$

In a previous study [20], a mapping of the displacement of the membrane was established and it was found at the center of the membrane (r = 0) a maximal deflection of 39.2 µm (U_{max}), for a mechanical excitation of 60 Hz. Consequently, equation #1 can be converted as follow:

$$U_Z(r=0) = U_{max} = \frac{P}{64D}\left(R^4\right) \quad (2)$$

Combining the equations #1 and #2, the displacement of the membrane (Uz) on each node was represented by the following equation:

$$U_Z(r) = U_{max}\left(2 + \frac{r^4}{R^4} - \frac{2r^2}{R^2}\right) \quad (3)$$

The FE element model of the phantom (Fig. 2D) was modeled as a 3D homogeneous, isotropic cylinder (diameter: 25 cm and height: 5 cm) and different densities, close to the liver tissue, were tested (range: 900 kg/m^3 to 1100 kg/m^3) in order to obtain the best propagation of the shear wave. The finite element mesh was composed of C3D8R (8-node linear brick) elements and different mesh sizes (2 mm, 5 mm, and 10 mm) were also performed in order to optimize the calculation time. In addition, due to the assumption that the phantom is almost incompressible (ν = 0.5), different Poisson's ratios (0.49, 0.495, and 0.499) were applied in order to optimize the shear wave displacement. According to the liver stiffness referenced in the literature (Huwart et al., 2008) for healthy and pathological liver tissue, the elastic properties of the phantom, represented by the Young's modulus ($E_{\_Phantom}$), varied from 0 kPa to 30 kPa (E = 3µ therefore 0 < µ < 10 kPa,) with an increment of 0.1 kPa.

The FE membrane and the FE phantom models (Fig. 2E) were combined using a tie constraint in order to observe the propagation of the shear wave through the plastic phantom. To reduce the time resolution (CPU time) of the 3D finite element model, a 2D cross-sectional FE model (Fig. 2E) (always composed of the membrane and the phantom) associated with an

axisymmetric assumption was performed. The dimensions and the mechanical properties of the 2D cross-sectional FE model were the same as those constituted by 3D FE model, excepted for the mesh definition of the membrane and the phantom represented by MAX1(2-node linear axisymmetric membrane) and CAX4R (4-node bilinear axisymmetric quadrilateral) elements, respectively.

2.3 Finite element analysis and identification process

To visualize the propagation of the shear wave, the FE model was analyzed with a dynamic implicit analysis, and the total time was fixed to 200 ms with a time increment of 1 ms (Fig. 2F). The material damping was assumed to be zero. The simulated propagation of the shear wave was visualized after nine periods in order to obtain similar wave behavior as the one experimentally obtained through the phantom with the MRE technique. Similar to the MRE post processing (Fig. 2B), a profile was manually placed along the simulated shear wave propagation in order to visualize the simulated wave displacement along the profile (Fig. 2G).

2.4 Identification process

The identification process (Fig. 2H) was made with a cost function (J, mm^2) related to a least squared analysis based on the relative error between the experimental ($Displacement\_{MRE}$) and the 2D numerical ($Displacement\_{FEM}$) wave displacements, represented by the grey surface (Fig. 2H).

Then, the optimization loop was performed and the cost function values were recorded and plotted as a function of the shear stiffness in order to identify the minimum value revealing the optimal elastic properties of the phantom (Fig. 2I).

III. RESULTS

3.1 In vivo and in vitro stiffness measurement with MRE technique

In vivo phase images, recorded during the MRE liver exam, represent the propagation of the shear wave obtained for a healthy (Fig. 1B) and a fibrotic (Fig. 1C) liver. The pathological liver, being constituted of stiffer tissue, revealed an increase of the wavelength inducing an increase of the stiffness compared to healthy liver. The shear stiffnesses for the present cohort of healthy and fibrotic livers were 1.79 ± 0.06 kPa and 4.92 ± 1.42 kPa, respectively.

In vitro phase images of the phantom (Fig. 2B) were obtained with the same boundary conditions (frequency: 60 Hz, displacement of the liver driver membrane) as the liver MRE test. The displacement of the shear wave through the phantom was clearly propagated and the measurement of the wavelength revealed a shear stiffness (μ) of 4.16 ± 0.14 kPa.

3.2 Influence of mesh, Poisson's ratio, and density on the FE phantom model

The optimized size for the C3D8R elements constituting the finite element mesh of the phantom was 5 mm. Indeed, the result of the calculation time was increased for elements of 2 mm (≈ 28000 s) compared to elements of 5 mm (≈ 918 s). To further reduce the calculation time using the 5 mm elements, the identification process was performed on a 2D finite element model leading to a final calculation time of only 9 s. Moreover, the similar wave displacement behavior obtained between the 2D and 3D finite element models validates the use of the 2D simplified model with a rotational symmetry.

The comparison between the numerical wave displacements (obtained from the three different Poisson's ratios (Fig. 3A) and densities (Fig. 3B)) and the experimental propagation revealed that the optimal Poisson's ratio and density were 0.499 (Fig. 3A) and 1000 kg/m^3 (Fig. 3B).

3.3 Optimization of the numerical shear wave displacement

To visualize the simulated propagation of the shear wave within the phantom, the increment time for the finite element analysis must be smaller than the period (16.6 ms) corresponding to the mechanical excitation (60 Hz). Thus, the optimal increment was found for 1 ms. In addition, the visualization of the simulated shear wave propagation was performed at different times (from 150 ms to 167 ms) in order to identify the optimal time revealing the entire representation of the shear wave behavior. The results revealed an optimal time of 163 ms corresponding to 9.75 periods.

3.4 Comparison of the experimental (MRE) and numerical (FE) shear wave displacement

The results of the identification process revealed a minimum of the cost function ($J = 6.49x10^{-4}$ mm²) for a Young's modulus of 12.1 kPa, or a shear stiffness of 4.03 kPa (Fig. 4). The computational time, to obtain all values of the cost function, was approximately 9000 s. The comparison between the experimental (MRE) and numerical (FE) shear stiffness (μ) showed a relative error of 3.1%.

IV. DISCUSSION

Magnetic resonance elastography (MRE) is a new non-invasive clinical exam prescribed in Europe and the United States [21] which improves the diagnosis and treatment of liver disorders and cost-effective prevention. In a previous study [20], the material properties of the clinical liver driver (excitation of the membrane) were determined in order to define the most adapted frequency for a liver test. To further apply this technique for the characterization of other soft tissues (kidney, spleen, psoas) [24] *in vitro* MRE tests were performed on phantoms, allowing the set-up of new MRE protocols and to assess its feasibility. Thus, a phantom was created with a stiffness (about 4kPa) corresponding to different biological tissues such as healthy muscle in a relaxed state [3], healthy spleen [24], or fibrotic liver [7].

Therefore, the continuity of this work was to simulate the MRE shear wave propagation, through the developed phantom, using a finite element model. The originality of this study was to develop a finite element composed, for the first time, of the realistic MRE liver boundary conditions. Indeed, the sinusoidal displacement induced by the clinical liver driver was quantified with a vibrometer analysis [20]. At that time, MRE studies were currently simulated using unrealistic *in vivo* boundary conditions such as a fixed harmonic displacement (10 µm) applied to the bottom surface of the model [12], an unknown displacement performed at the node located in the middle of the top surface [18,19], a sinusoidal force made tangent to the top surface [11], a uniform displacement of 1.5 mm set on the outer surface nodes [25] or a sinusoidal shear load (2 kN) applied to the nodes [13].

In addition to the realistic boundary condition, the simulated propagation of the shear wave is also highly influenced by the material properties of the phantom such as its elasticity, viscosity, density and its Poisson's ratio. Since liver tissue is considered to be nearly incompressible and mainly constituted of water, the present study took care in testing various values of density and Poisson's ratios in order to develop the closest FE phantom model

possible for mimicking liver tissue. In addition, the hepatic tissue, as well as other biological tissues, was characterized with a viscoelastic behavior. In the present study, the finite element model of the phantom was composed with only elastic properties revealing the global elasticity of the tissue using the linear elastic assumption in ABAQUS software. This choice was based on the relevance of this parameter compared to the viscous one which represents the micro structural changes. Moreover, in the literature [16,18,19,25] most of the MRE finite element models were developed with only the elastic properties, and only one study used the viscoelastic assumption for the brain with COMSOL software [11]. In the future, it will be of interest to develop a finite element model with the realistic viscoelastic properties of the liver and to analyze the effect of the viscous component on the shear wave propagation. Furthermore, in case of a more complex finite element model, the use of a genetic algorithm will be necessary to more rapidly identify the optimal mechanical properties from the minimization of the cost function.

The similar experimental (MRE) and numerical (FE) shear wave displacements validate the present identification process performed on a phantom which is comparable to a fibrotic liver. This study provides experimental and numerical data related to MRE technique which could be used in the future as a starting point for the development of finite element models mimicking various abdominal tissue behaviors. The perspective of this entire study will be to supplant the phantom by a reconstructed hepatic gland in order to validate the present identification process on an *in vivo* liver tissue.

ACKNOWLEDGEMENTS

Competing interests: None declared

Funding: Picardie Region

Ethical approval: The study was approved by the Institutional Review Board, “Comité de Protection des Personnes Nord-Ouest II” (ref : 2008-A00524-51)

References

[1] Zuberi S, Matta N, Nawaz S, Stephenson J, McWilliam R, Hollman A. Muscle ultrasound in the assessment of suspected neuromuscular disease in childhood. Neuromuscular Disorders 1999;9:203–7.

[2] Van Beers B, Doblas S, Sinkus R. New acquisition techniques: fields of application. Abdominal Imaging 2012;37:155–63.

[3] Bensamoun SF, Stevens L, Fleury MJ, Bellon G, Goubel F, Ho Ba Tho M-C. Macroscopic–microscopic characterization of the passive mechanical properties in rat soleus muscle. Journal of Biomechanics 2006;39:568–78.

[4] Bensamoun SF, Wang L, Robert L, Charleux F, Latrive J-P, Ho Ba Tho M-C. Measurement of liver stiffness with two imaging techniques: Magnetic resonance elastography and ultrasound elastometry. Journal of Magnetic Resonance Imaging 2008;28:1287–92.

[5] Shinohara M, Sabra K, Gennisson J, Fink M, Tanter M. Real time visualization of muscle stiffness distribution with ultrasound shear wave imaging during muscle contraction. Muscle & Nerve 2010;42:438–41.

[6] Niitsu M, Michizaki A, Endo A, Takei H, Yanagisawa O. Muscle Hardness Measurement by Using Ultrasound Elastography: A Feasibility Study. Acta Radiol 2011;52:99–105.

[7] Huwart L, Sempoux C, Vicaut E, Salameh N, Annet L, Danse E, Peeters F, ter Beek LC, Rahier J, Sinkus R, Horsmans Y, Van Beers BE. Magnetic Resonance Elastography for the Noninvasive Staging of Liver Fibrosis. Gastroenterology 2008;135:32–40.

[8] Mazza E, Grau P, Hollenstein M, Bajka M. Constitutive modeling of human liver based on in vivo measurements. Medical Image Computing and Computer-Assisted Intervention 2008;11:726–33.

[9] Nava A, Mazza E, Furrer M, Villiger P, Reinhart WH. In vivo mechanical characterization of human liver. Medical Image Analysis 2008;12:203–16.

[10] Sack I, Bernarding J, Braun J. Analysis of wave patterns in MR elastography of skeletal muscle using coupled harmonic oscillator simulations. Magnetic Resonance Imaging 2002;20:95–104.

[11] Atay SM, Kroenke CD, Sabet A, Bayly PV. Measurement of the Dynamic Shear Modulus of Mouse Brain Tissue In Vivo by Magnetic Resonance Elastography. Journal of Biomechanical Engineering 2008;130:021013.

[12] Clayton EH, Garbow JR, Bayly PV. Frequency-dependent viscoelastic parameters of mouse brain tissue estimated by MR elastography. Physics in Medicine and Biology 2011;56:2391–406.

[13] Thomas-Seale LEJ, Klatt D, Pankaj P, Roberts N, Sack I, Hoskins PR. A Simulation of the Magnetic Resonance Elastography Steady State Wave Response through Idealised Atherosclerotic Plaques. IAENG International Journal of Computer Science 2011;38:2636–9.

[14] Muthupillai R, Lomas DJ, Rossman PJ, Greenleaf JF, Manduca A, Ehman RL. Magnetic Resonance Elastography by Direct Visualization of Propagating Acoustic Strain Waves. Science 1995;269:1854–7.

[15] Litwiller DV, Lee SJ, Kolipaka A, Mariappan YK, Glaser KJ, Pulido JS, Ehman RL. MR elastography of the ex vivo bovine globe. Journal of Magnetic Resonance Imaging 2010;32:44–51.

[16] Chen Q, Bensamoun SF, Basford JR, Thompson JM, An K-N. Identification and Quantification of Myofascial Taut Bands With Magnetic Resonance Elastography. Archives of Physical Medicine and Rehabilitation 2007;88:1658–61.

[17] Glaser KJ, Felmlee JP, Ehman RL. Rapid MR elastography using selective excitations. Magnetic Resonance in Medicine 2006;55:1381–9.

[18] Chen Q, Ringleb SI, Manduca A, Ehman RL, An K-N. A finite element model for analyzing shear wave propagation observed in magnetic resonance elastography. Journal of Biomechanics 2005;38:2198–203.

[19] Chen Q, Ringleb SI, Manduca A, Ehman RL, An K-N. Differential effects of pre-tension on shear wave propagation in elastic media with different boundary conditions as measured by magnetic resonance elastography and finite element modeling. Journal of Biomechanics 2006;39:1428–34.

[20] Leclerc GE, Debernard L, Foucart F, Robert L, Pelletier KM, Charleux F, Ehman R, Ho Ba Tho M-C, Bensamoun SF. Characterization of a hyper-viscoelastic phantom mimicking biological soft tissue using an abdominal pneumatic driver with magnetic resonance elastography (MRE). Journal of Biomechanics 2012;45:952–7.

[21] Nguyen D, Talwalkar JA. Noninvasive assessment of liver fibrosis. Hepatology 2011;53:2107–10.

[22] Ehman RL, Rossman PJ, Hulshizer TC, Dresner AM. Pressure activated driver for magnetic resonance elastography. U.S. Patent 20050270029, 2005.

[23] Trotignon J-P, Piperaud J, Verdu J, Dobraczynski A. Precis de matières plastiques: structures, propriétés, mise en oeuvre et normalisation. Courbevoie; Paris: AFNOR, Nathan; 1982.

[24] Bensamoun SF, Robert L, Leclerc GE, Debernard L, Charleux F. Stiffness imaging of the kidney and adjacent abdominal tissues measured simultaneously using magnetic resonance elastography. Clinical Imaging 2011;35:284–7.

[25] McGrath DM, Foltz WD, Al-Mayah A, Niu CJ, Brock KK. Quasi-static magnetic resonance elastography at 7 T to measure the effect of pathology before and after fixation

on tissue biomechanical properties. Magnetic Resonance in Medicine 2011:DOI: 10.1002/mrm.23223.

Figure legends

Fig. 1. In vivo MRE liver exam performed on a healthy subject and a patient with a fibrotic liver.

Fig. 2. Identification process based on the comparison of the shear wave propagation obtained experimentally, with the magnetic resonance elastography (MRE) technique, and numerically with the development of a finite element model. The finite element models (phantom and membrane) were constituted with realistic MRE liver boundary conditions and similar material properties of fibrotic liver.

Fig. 3. Comparison of the experimental (MRE) and numerical (FE) wave displacements. Different Poisson's ratios (A) and density (B) were tested to find the most representative simulated wave behavior to the experimental one.

Fig. 4. Representation of the cost function (J, mm^2) as a function of the shear stiffness (μ, kPa), showing the result of the identification process.

Figures

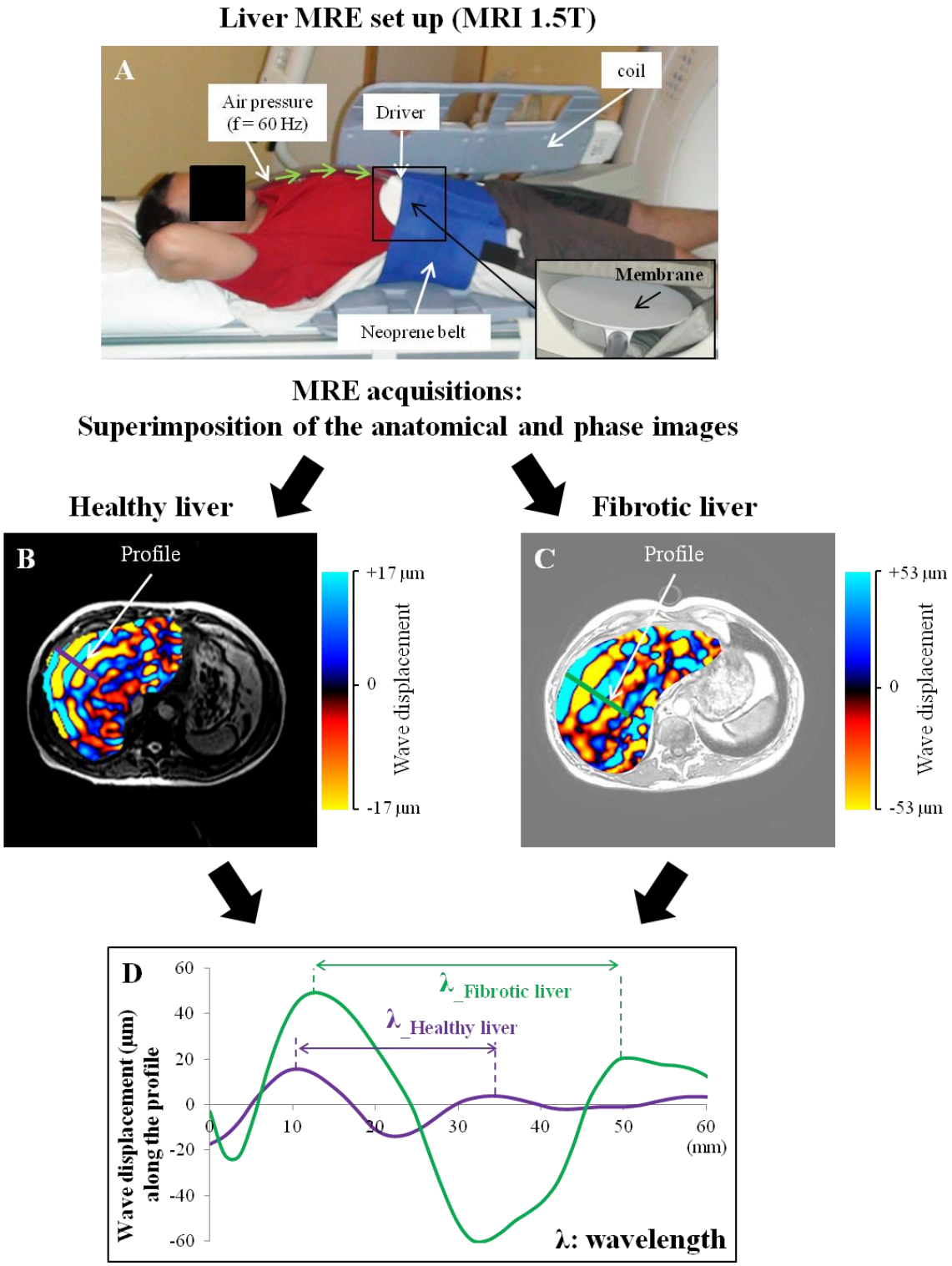

Fig. 1. In vivo MRE liver exam performed on a healthy subject and a patient with a fibrotic liver.

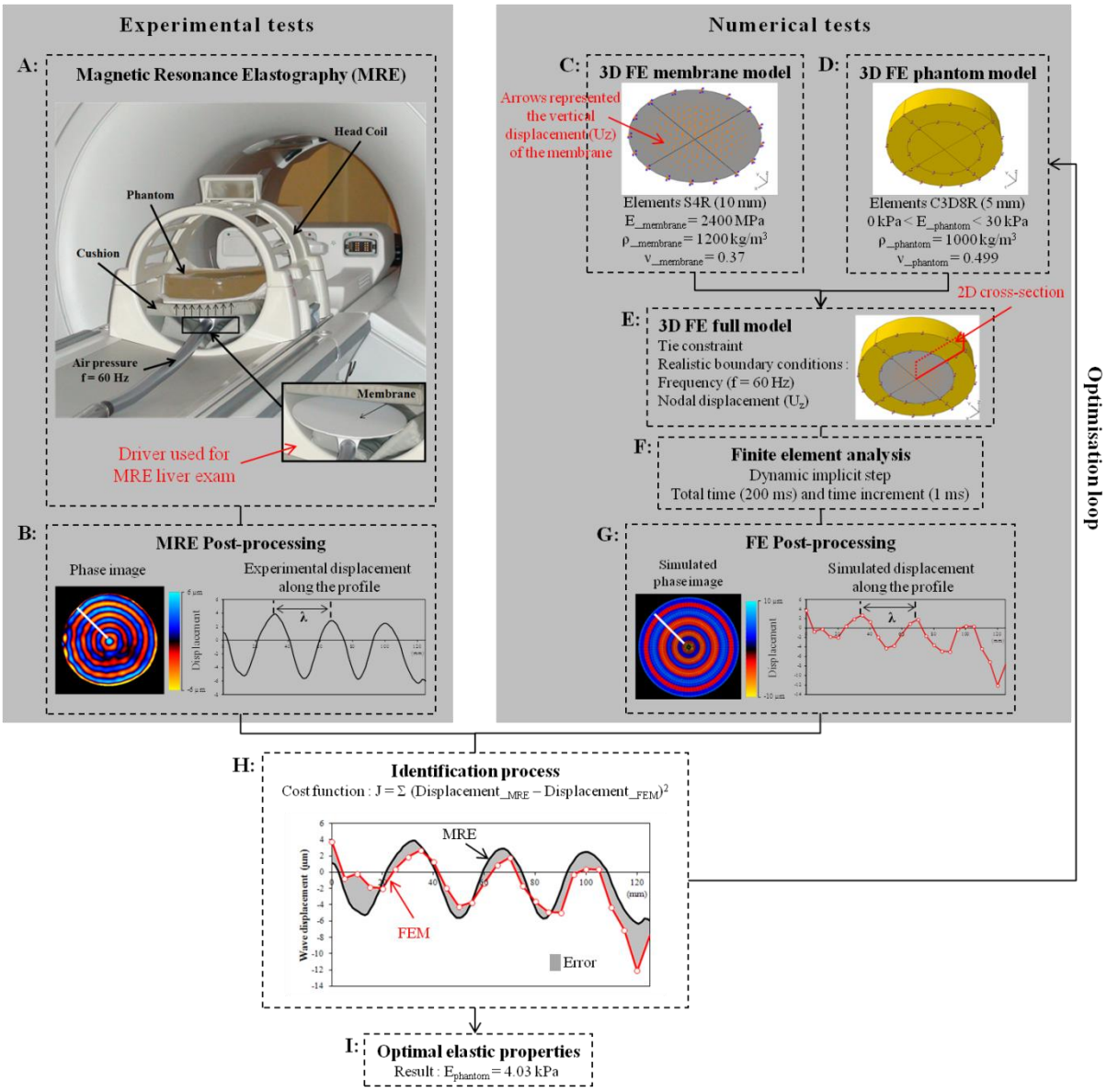

Fig. 2. Identification process based on the comparison of the shear wave propagation obtained experimentally, with the magnetic resonance elastography (MRE) technique, and numerically with the development of a finite element model. The finite element models (phantom and membrane) were constituted with realistic MRE liver boundary conditions and similar material properties of fibrotic liver.

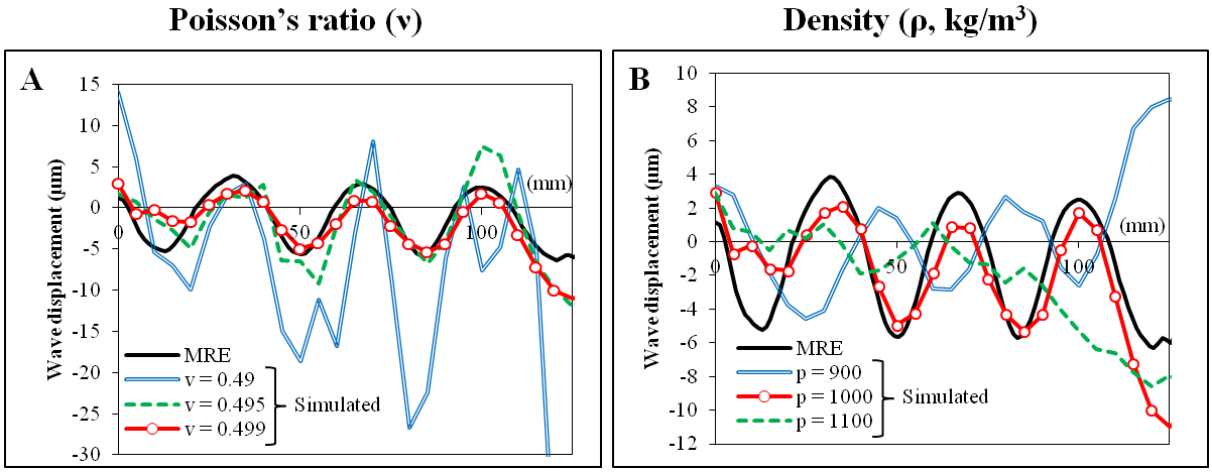

Fig. 3. Comparison of the experimental (MRE) and numerical (FE) wave displacements. Different Poisson's ratios (A) and density (B) were tested to find the most representative simulated wave behavior to the experimental one.

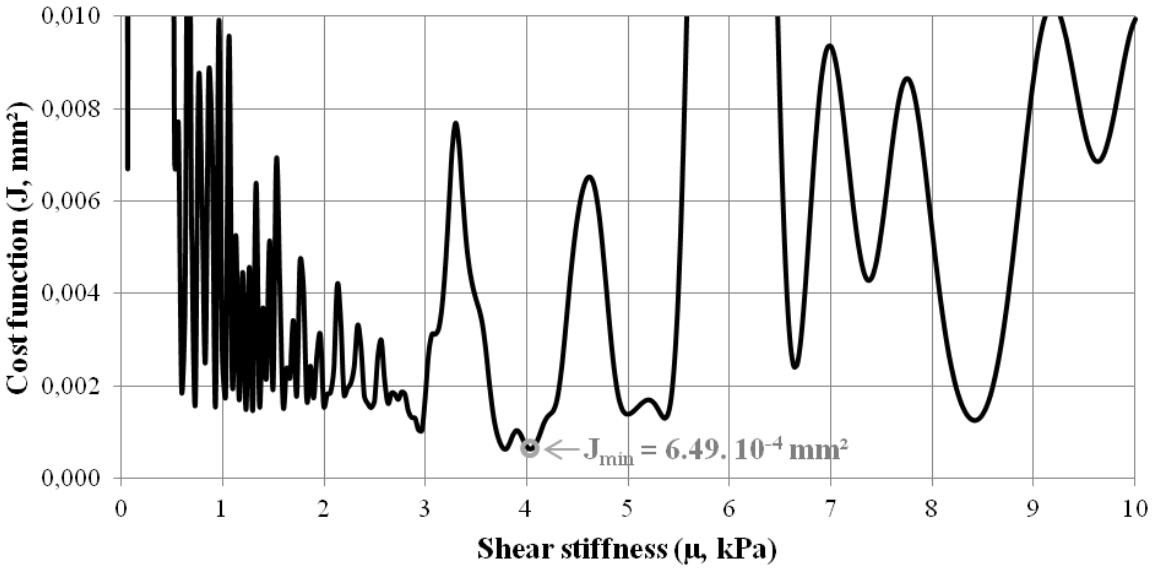

Fig. 4. Representation of the cost function (J, mm²) as a function of the shear stiffness (μ, kPa), showing the result of the identification process.